Frontiers in Pharmacological Research
Volume 2 Issue 1 2026

Frontiers in Pharmacological Research
Volume 2 Issue 1 2026

Optimizing 3D spheroid monoculture and co-culture models of breast cancer for pharmaceutical investigation and screening

Suárez, José, de Medina

Department of Pharmacological Research

Article Info

Received: 20-12-2025 Revised:21-1-2026 Accepted:23-2-2026 Published:26-3-2026

Abstract

BACKGROUND: Test methods utilized in preclinical cancer medication development must have reproducibility and physiological relevance. In this regard, the ability of 3D cell culture models, such as spheroids or organoids, to replicate natural biology has recently made them appealing. Additionally, complete automation of sample preparation and data processing is crucial to boosting screening efficiency and throughput.OBJECTIVE: This work addressed spheroid cell culture methodological factors, such as media composition, extracellular matrix, addition of stromal cells, and quality of contrast-based readouts, that are particularly relevant for reproducibility and physiological significance in studies investigating metabolic effects of drug treatment.

METHODS: MCF10A human breast epithelial cells and MDA-MB-231 human breast cancer cells were used to create spheroids using standardized and enriched medium along with extra basal membrane extract. Additionally, MDA-MB-231 and CCD-1137Sk human fibroblast cells were co-cultured to create spheroids. The metabolic behavior of the samples was compared. Western blotting, confocal microscopy, and SpheroidSizer software were used in spheroid analysis. RESULTS: The co-culture environment, supporting additives, and media composition can significantly change the development and metabolic behavior of spheroids. Specifically, the presence of extracellular matrix components and prolonged culture had an impact on spheroid integrity. Automated spheroid size analysis data required careful consideration because of drug- or culture-induced spheroid disintegration.

Conclusion: For standardized spheroid-based drug screening methods, media composition, extracellular matrix, stromal cell addition, and automated readouts are crucial factors. In automated high-throughput screens, contrast-based spheroid size assessments require extra care since spheroid-disaggregation or surrounding cell growth may complicate the readouts.

Keywords: automation, multicellular spheroids, breast cancer, cell culture, co-culture, high-throughput screening techniques, and tumor cell lines

Overview

Reproducibility and physiological relevance are critical components of successful preclinical cancer therapy research and the basis of successful clinical trials for therapeutic launches. Unfortunately, the ratio of approvals per medicine entering phase-I clinical trials decreased steadily from 17% between 1995 and 2000 [1] to 5% in 2013. 409 of the 7,872 drugs that entered clinical testing during that year were approved. With 733 approvals out of 5,315 trial candidates in 2015, the success rate was recently rising once more, reaching 13.8% [2]. This was likely caused by greater efforts in the early phases of drug development, such as

increased use of biomarkers in drug target screenings. However, the average time and cost of developing a new, commercially viable cancer medication have continued to increase recently, reaching 7.3 years (range 5.8–15.2 years) and 757 million USD, respectively [3]. These figures demonstrate how much room there is for advancements in drug development processes. Furthermore, both basic and applied research would benefit from reproducibility and comparability. However, research studies frequently employ highly specialized approaches, making it difficult to compare their findings.

The MDA-MB-231 cell line was created in 1973 from a female patient with triple-negative breast cancer who had experienced a metastatic relapse following a mastectomy four years prior. Compared to other breast cancer cell lines, these cells have a moderate doubling time [4].

Since then, their culture has been carried out using a variety of medium compositions without a clear standard. Initially, 15% fetal calf serum (FCS), glutathione, gentamicin, insulin, and Leibovitz L15 medium was employed to cultivate MDA-MB-231 cells in air at 37°C [4]. Even though using 5% CO2 has become the norm, there are still a variety of media compositions, such as changes in the concentration of FCS (10–20%), insulin (0–10 µg/mL), glutamine (0–2 mM), and antibiotics (carbenicillin, gentamicin, amphotericin, penicillin, and streptomycin). Additionally, more popular variations like DMEM or RPMI1640 have replaced Leibovitz L-15 as the basal medium [5–9]. However, because they may contain other amino acids, such as L-glutamine, their composition might vary from supplier to supplier [10, 11]. Lastly, the added serum, which is primarily FCS in MDA-MB-231 cultures, is known to vary. Since serum contains important factors that change cell proliferation [12], differentiation [13], and attachment [14], this could easily affect cellular behavior [4]. Sera exhibit intrinsic variety because they are complex natural molecules [15]. Co-culturing various cell lines influences cell survival and differentiation by altering the availability of signals and factors [16]. Cell-cell interactions have been recognized to change in vitro cell cultures since the 1960s [17]. Co-cultures have therefore always been a preferred experimental strategy to more accurately replicate the physiological state in cell culture models. However, because monocultures are easier to standardize, they are more frequently employed to assess things like proliferative effects [18], medication sensitivity of a tissue entity [19], or the ability for cancer cells to spread [20]. On the other hand, compared to controls using single cell types, co-culturing can disclose crucial cell-cell communication and result in unexpected cellular responses [21]. For instance, the segregation of extracellular matrix components caused by co-cultures of osteoblasts and peripheral blood mononuclear cells made it possible to substitute growth factor supplementation for bone regeneration [22]. Targeting the tumor microenvironment rather than just the cancer cells produced better treatment outcomes in co-cultures of fibroblasts and cancer cells [23]. This implies that cancer-associated fibroblasts, which sustain tumor cells by supplying metabolites and changing the tissue composition [24–26], ought to be taken into account as potential targets for medication.Although 2D cell culture models were favored for many years because they were inexpensive and simple to prepare, interest in 3D cell culture models has recently increased because of their potential to more closely resemble physiological circumstances [27]. In particular, in 3D cultures, the access of nutrients and oxygen [28], cellular interactions [29], mechanistic support [30], and the permeability of drugs [31–33] are more similar to that in tumors than in classical 2D cultures. Consequently, three-dimensional research is beneficial for these characteristics [34].Spheroid cultures are frequently difficult to cultivate for extended periods of time because of their sensitivity to mechanical stress [35]. Additionally, they usually show detached or dispersing cells that are not part of the core spheroid [36]. This heavily depends on how the civilizations' three-dimensional structures were developed [37]. Finally, three-dimensional cell culture in general has two major drawbacks: it is more time consuming and expensive compared to 2D cultivation [38]. Operative automation is therefore desired. Depending on the size of enterprise, this involves cell culture handling, drug treatment, data acquisition, and segmentation-based data evaluation. While data quality is increasing continuously, automated 3D readouts based on 2D data achieved with widefield microscopy can lead to erroneousdata interpretation. For example, the calculation of spheroid size based on simple image thresholding might overlook effects of cellular dissemination and spheroid disintegration [39–41].

Materials and methods

Cell culture

Dulbecco's Modified Eagle Medium (Capricorn, DMEM-HPA, Lot# CP18-2096) supplemented with 10% fetal bovine serum (Capricorn, FBS-12B, Lot# CP16-1422), 1% Minimum Essential Medium Nonessential Amino Acids (Capricorn, NEAA-B, Lot# CP17-1726), and 1% penicillin/streptomycin (Capricorn, PS-B, Lot# CP18-2207) were used to pass MDA-MB-231 human breast cancer cells. IMDM containing Iscove's Modified Dulbecco's Medium (Capricorn, IMDM-A, Lot # CP18-2245) supplemented with 10% FBS-12B and 1% PS-B was used to passage CCD-1137Sk human foreskin fibroblasts. 5% horse serum (Gibco, Gibco HI Horse Serum, #26050088), 20 ng/mL epidermal growth factor (Miltenyi, EGF, #130.093.825), 500 ng/mL hydro-cortisone (Sigma, H-0888, Lot# 86H04185), 100 ng/mL cholera toxin (Sigma, C8052-0.5MG, Lot# 116M4078) made up MCF-M. MDA-MB-231 and CCD-1137Sk were seeded with 1 × 106 cells per T75 flask, whereas MCF10A was planted with 5 × 106 cells. All cell lines were passaged at 80% confluency. Using 96-well spheroid microplates (Corning, Ref 4520, Lot# 04618014), spheroid formation was accomplished by adding the proper quantity of cells and centrifuging at 500 rcf for 6 minutes. Before centrifugation, if necessary, 2.5% of basement membrane extract (BME/Cultrex, PathClear No. 3432-005-01, Lot# 41651B18) was applied just after the cells. Twelve replicates were made for every data point.

1.2. Brightfield microscopy and assessment of spheroid size

The Axiovert 25 (Zeiss, objective CP-ACHROMAT, 5x/0.12Ph0) was used to take brightfield images for spheroid size estimation. The images were exported in TIFF format for additional processing, and MATLAB's SpheroidSizer program was used for analysis [41].

1.3. Confocal microscopy and immunostaining

Phosphate-buffered saline (PBS) containing 4% paraformaldehyde (PFA) was used to fix cell cultures for thirty minutes. The samples were blocked using 3% bovine serum albumin fraction V (BSA) in deionized water following permeabilization with 0.4% Triton-X100 in deionized water. The primary antibody was incubated at 4◦C for the entire night. Secondary antibodies and dyes were applied for two hours at room temperature following PBS washing. Wheat germ agglutinin (WGA/Biotium, CF488A, #29022) was diluted 1:500 and 2-(4-Amidinophenyl)-6-indolecarbamidine dihydrochloride (DAPI/Roche, 10236276001, Lot# 28114320) was diluted 1:1000. PTEN (Proteintech, AB9260, Lot# 2; 1:100), MCT4 (SantaCruz Biotechnology, sc-376140, Lot# D3018; 1:400), LC3 (CellSignalling, 3868 S, Lot# 11; 1:200), and KI67 (Merck, AB9260, Lot# 3094997; 1:500) were the primary antibodies. Goat anti-Rabbit 647 (Invitrogen, A21246, Lot # 55002A) and goat anti-Mouse alexa fluor 488 (Invitrogen, A11001, Lot # 1834337) secondary antibodies were diluted 1:1000. An inverted Leica SP8 (Leica Microsystems) fitted with HC PL APO 20 × /0.75 IMM CORR and HC PL APO CS2 63 × /1.2 W CORR lenses was used for confocal microscopy. The visualization was made usingthe Leica LAS-X 3.3.0 software suite and the image capturing was set to 1024 × 1024 pixels resolution with 3 times frame average and a pinhole of 1 airy units. Z-step size in 3D stacks was 1 µm. All images used for direct comparison were taken at the same day with identical settings of laser, gain and pinhole.For the quantification of specific signals, the overall intensity divided by the total area was normalized on the supplement-rich MCF-M without added BME while seeding.

Western blotting

Protein extraction was achieved with 1 h incubation of trypsinated cells in lysis buffer (50 mM Tris-HCl, 150 mM NaCl, 1% NP-40

(AppliChem, A1694) with 10% glycerol, 1 mM EDTA, 1 mM EGTA, 1x protease inhibitor cocktail (Roche, #88665) and 0.5 mM PMSF (AppliChem, A0999) on ice), before heating to 99°C for 7 min after addition of Laemmli buffer. The amount of protein was measured with a BCA assay (ThermoScientific, 23225, Lot# SI256196) and 30 µg of each probewere subjected to a 10% SDS-PAGE followed by Western blot analysis. The used primary antibodies were specific for light-chain 3 (1:1000/LC3/rabbit anti-LC3B mAb/Cell Signaling, #3868 S, Lot# 11) or Glyceraldehyde-3-phosphate dehydrogenase (1:10000/GAPDH/mouse anti-GAPDH mAb/Thermo Fisher, MA5-15738). Secondary antibodies were diluted 1:10000 and goat anti-rabbit IgG (H+L) HRP (Jackson Immuno Research, 111035003) together with goat anti-Mouse IgG (H+L) HRP (Thermo Fisher, #32430) were utilized.

Gels were developed with Western Bright Chemilumineszenz Substrat Sirius (Biozym, 541020, Lot# 180829), pictures captured with a G:Box (Syngene, model Chemi XX6) and evaluated using ImageJ software (v1.48v). Biological triplicates were made and each data point was technically analyzed three times.

Statistics

For statistics, GraphPad Prism 7 was used applying one-way ANOVA and multiple comparison based on the raw data. Normal distribution and homoscedasticity were tested using Kruskal-Wallis and F-test, respectively. All graphs show mean values and standard deviation. Significance was as indicated ($^{*}p < 0.05$, $^{****}p < 0.0001$).

Results

Media assays were conducted with each cell line to assess the impact of various media on the spheroid growth of highly metastatic MDA-MB-231 breast cancer cells and non-tumorigenic MCF10A breast gland epithelial cells. These studies involved incubation in MDA-M and MCF-M medium that were either sparsely or generously supplied, as well as in the presence or absence of BME extracellular matrix substance. Brightfield microscopy showed significant variations across all culture conditions. First, compared to MCF10A cell-based spheroids, MDA-MB-231 spheroids were often bigger and more compact (Fig. 1A and C). MDA-MB-231 spheroids were fully spherical and solid in the presence of BME (Fig. 1A), whereas MCF10A cultures developed core spheroids with several satellite spheroids surrounding them (Fig. 1C). Both cell lines' spheroids were significantly smaller in the absence of BME, and the cultures had a large number of dispersed cells. Additionally, in generously supplemented MCF-M, both cell lines showed the highest growth (Fig. 1B and D; Table 1). According to this research, ECM components and metabolically relevant supplements have a synergistic influence on the development and compactness of spheroids.

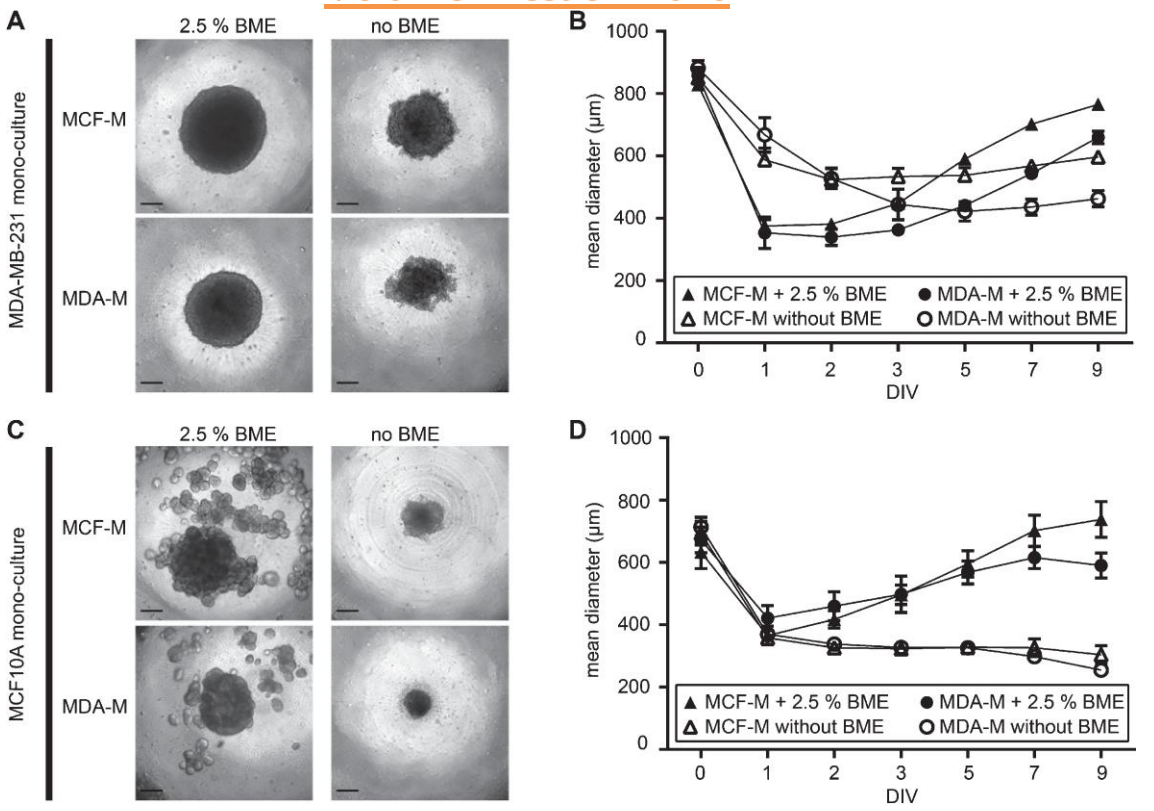

Fig. 1. Supplements of media and extracellular matrix components massively alter compactness and growth of breast cancer and epithelial spheroid cultures. MDA-MB-231 breast cancer and MCF10A breast epithelial cells were cultured in ultra-low attachment plates for up to 9 DIV using either rich media designed for MCF10A cells (MCF-M) or poor media for MDA- MB-231 cells (MDA-M) and in the absence or presence of BME.

(A) and (C), brightfield micrographs of MDA-MB-231 (A) or MCF10A (C) after 9 DIV. Scale bars, 200 µm. (B) and (D), quantitative analysis of spheroid-areas. Depicted are mean areas ± SD as a function of DIV. For each data point, at least 12 spheroids were analysed.MDA-MB-231 spheroids cultivated under these various conditions were stained for the marker protein Phosphatase and Tensin Homolog (PTEN) in order to examine the impact of media composition on spheroid growth from a metabolic perspective. This protein often correlates inversely with cellular activity because it is a negative regulator of the phosphoinositide 3-kinase Akt (PI3K/Akt) signaling pathway [42]. Immunofluorescence labeling of spheroids cultivated nine days in vitro (9 DIV) revealed, as predicted, varying levels of PTEN gene expression based on the medium composition and the presence of BME in the culture (Fig. 2). Spheroids grown in MCF-M without BME had the greatest values of PTEN fluorescence signal intensity per area, according to quantitative analysis. PTEN immunofluorescence signal intensities from cultures in MDA-M or MCF-M with BME achieved significantly lower amounts after normalizing this data point to 100%; specifically, 37.2% ± 4.4% (mean ± SD) or 42.0% ± 8.1% (mean ± SD), respectively. In conclusion, these findings imply that metabolically active supplements have both positive and negative effects on PTEN expression in

MDA-MB-231 spheroids.and by BME, in that order. We then conducted comparative tests of MDA-MB-231 mono-cultures and co-cultures with fibroblasts in order to get additional understanding of the impact of extracellular matrix components on MDA-MB-231 spheroid compactness and to evaluate the viability of co-culturing these cells with fibroblasts.

Comparison of mean diameters in 3D spheroid cultures at 9 DIV

between different culture conditions are shown in crossing fields.

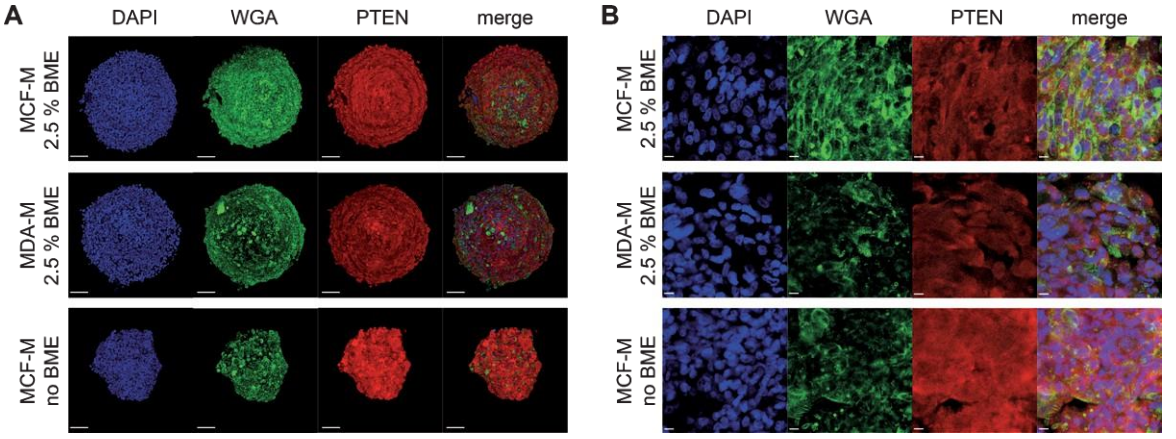

Fig. 2. Addition of BME strongly alters PTEN expression level in MDA-MB-231 spheroids. MDA-MB-231 cells were cultured in ultra-low attachment plates for 9 DIV using either rich media designed for MCF10A cells (MCF-M) or poor media for MDA-MB-231 cells (MDA-M) and in the absence or presence of BME. Then, whole mount spheroid staining was done using DAPI, WGA, and anti-PTEN antibodies to label nuclei (blue), cell membranes (green), and PTEN protein (red). Spheroids were then imaged using confocal microscopy. Panels depict maximum-z projections (A) or single optical slices

(B) from samples as indicated.

BME's existence or absence. We initially searched for seeding densities that produced roughly similar spheroid areas immediately following condensation and just prior to the linear development phase, i.e., at 4 DIV, in order to identify an experimental paradigm that permits quantitative comparisons. Each well was evaluated with 125–16,000 seeded cells. Co-cultures of MDA-MB-231 cells with fibroblasts were notably smaller than similar MDA-MB-231 mono-cultures employing the same numbers of MDA-MB-231 cells for all used cell densities. This showed that the optimal seeding density for monocultures was 8,000 cells per well, while for co-cultures of MDA-MB-231 and CCD-1137Sk, it was 10,000 cells each type (a total of 20,000 cells). A thorough examination of spheroids following 4, 7, 14, and 21 DIV showed distinct variations in long-term cultivation (Fig. 3A). MDA-MB-231 plus fibroblast co-cultures supported spheroid formation in the absence of BME (Fig. 3A), but despite the higher initial seeding density, the co-culture spheroids were growing more slowly and into significantly smaller cores (Fig. 3C) with many surrounding disseminating cells (Fig. 3A). In contrast, MDA-MB-231 mono-cultures supplemented with BME produced firm and stable spheroids with consistent growth for at least two weeks (Fig. 3A and C).

Monoculture spheroids were brittle and had a large number of dispersed or disintegrated cells when BME was not present (Fig. 3A). In these two settings, automated spheroid area recognition based on brightfield picture contrast revealed larger spheroid regions than manual segmentation due to the observed dispersal or dissociation effects (see Fig. 3B for an example of co-culture analysis). As DIV increased, so did the disparity between the surrounding dissociated cells and the core spheroid. As a result, the spheroid integrity, which is calculated by dividing the manually segmented core spheroid area by the automatically segmented area, dramatically declined over time, particularly for co-cultures (Fig. 3D) and monocultures without BME (data not shown).
We examined the autophagic activity in MDA-MB-231 monocultures and MDA-MB-231 plus fibroblast co-cultures to see if co-culturing also had an impact on metabolic traits. Western blot examination of MDA-MB-231 and CCD-1137Sk in 2D mono- and co-cultures produced modified LC3-II bands after normalization to the loading control GAPDH (Fig. 4A). One of the main active components of autophagic cells is LC3-II [44]. Quantitative analysis supported this conclusion, showing that MDA-MB-231 cells and fibroblasts in monoculture produced ratios of 0.66 ± 0.02 and 0.72 ± 0.01, respectively, while co-cultivation of these cell types produced ratios of 1.47 ± 0.05 in 2D and 1.31 ± 0.03 in 3D spheroid cultures (Fig. 4A and B). The Western blot was confirmed by immunofluorescence labeling of LC3 and MCT4, a sign of increased lactate shuttling. information. With relative signal intensities of 60.4 ± 6.9% (MDA-MB-231) or 40.8 ± 4.4% (fibroblasts) for LC3 and 68.4 ± 6.7% (MDA-MB-231) or 24.2 ± 3.2% (fibroblasts) for MCT4, fluorescence micrographs from the co-culture model.

3. Conversation

For phenotypic drug testing, tissue-specific cell culture models are essential. In this regard, co-culturing cancer cells with stromal cells can improve the models' physiological relevance, for example, by achieving distinct cellular subpopulations that could influence drug resistance or growth rates throughout the entire culture [45, 46]. Moreover, 3D cultures are frequently thought to more closely resemble physiological circumstances [47]. Here, we discussed factors that can assist prevent undesired data heterogeneity between several experimental 3D cell culture paradigms. This demonstrated the importance of co-culture conditions, supporting additives, medium composition, and post-processing data analysis while setting up 3D cancer cell models. Initially, we concentrated on creating 3D spheroid models unique to breast tissue using either the non-tumorigenic breast epithelial cell or the human breast cancer cell line MDA-MB-231 [5]. Line

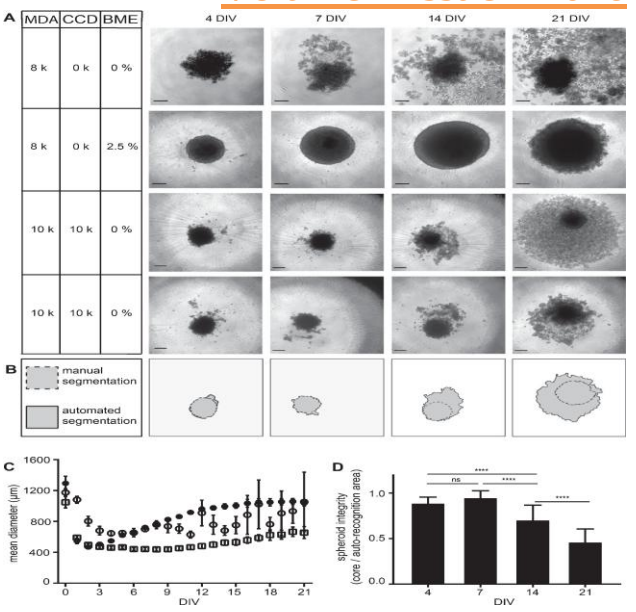

Fig. 3. MDA-MB-231 spheroid integrity is preserved in the presence of BME and partially also achieved by co-culturing with CCD-1137Sk fibroblasts. MDA-MB-231 breast cancer cells were either cultured alone in ultra-low attachment plates for up to 21 DIV using MDA-M in the absence or presence of BME or in co-culture with CCD-1137Sk human fibroblasts in the absence of BME. (A) Brightfield micrographs of spheroids at 4, 7, 14, and 21 DIV under culture conditions as indicated with cell lines MDA-MB-231 (MDA) and CCD-1137Sk (CCD) supplemented with basal membrane extract (BME). For co-cultures, two data sets are shown to illustrate the variability in spheroid disintegration. Scale bars, 200 µm. (B) Difference between automated (solid outline) and manual segmentation (dashed outline) using SpheroidSizer as illustrated on the lower
panels in (A). (C) Quantiative analysis of spheroid diameters as a function of DIV. Depicted are mean values ± SD. For each
data point, at least 12 spheroids were analysed. (D) Quotient of manually versus automatically segmented spheroid areas as a measure of spheroid integrity. Depicted are mean values ± SD. For each data point, at least 40 spheroids were analysed.

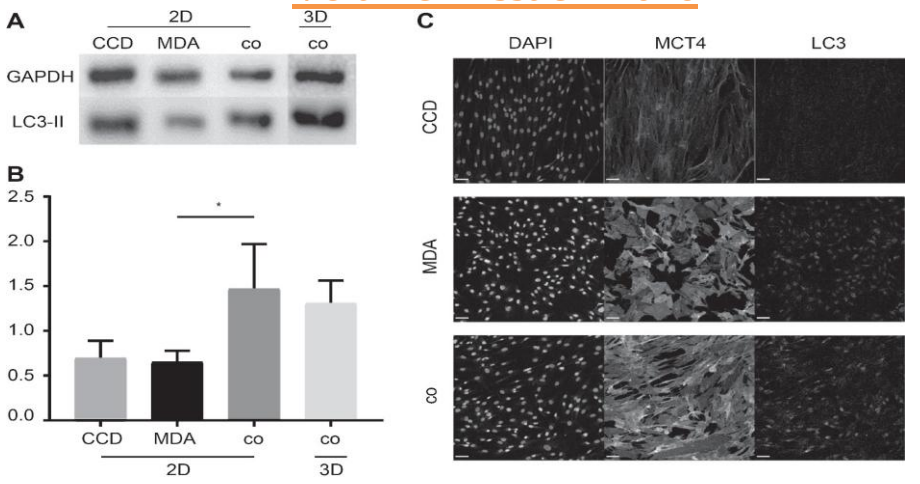

Fig. 4. Co-cultures of MDA-MB-231 and CCD-1137Sk cells exhibit higher levels of LC3-II and MCT4 expression. MDA- MB-231 breast cancer cells and CCD-1137 fibroblasts were either cultured alone as adherent cultures (2D) or co-cultured in 2D (2D) or in ultra-low attachment plates (3D) for 4 DIV. Then, cells were analysed by Western blot (A-B) or immunofluorescence
(C). (A) Representative Western blot bands upon staining against LC3-II or GAPDH. (B) Quantitative analysis of LC3-II band intensities upon normalization to GAPDH. Depicted are mean + SD. At least 3 experimental replicates were made. (C) Confocal images of representative 2D regions stained for nuclei (DAPI), MCT4, and LC3. Scale bars, 100 μm.

MCF10A [48]. Finding a media mix that would work for both cell lines would have made it possible to co-culture these cells and examine the effects of medications or other treatments on particular cell types. This demonstrated a substantial dependence of both cell types on the presence of BME in terms of spheroid integrity and size, while the supplementation with insulin and metabolism-stimulating substances seen in the MCF-M seemed to be less important but only caused minor size changes. This implies that co-cultures between MDA-MB-231 and MCF10A cells should be feasible after BME is added, possibly because it delivers extracellular matrix components or adds significant growth stimulation.

We continued to cultivate MDA-MB-231 cells as monocultures using various media compositions and assessed their metabolic activity, or we co-cultured them with fibroblasts that ought to be able to supply extracellular matrix in order to distinguish between these two possibilities. Regarding the first method, the results showed that the richness of the examined medium and PTEN expression were negatively correlated. These findings initially seemed counterintuitive because PTEN is a recognized down-regulator of the Akt/mammalian target of rapamycin (Akt/mTOR) signaling pathway, which is connected to active metabolism. Strong activating external inputs, however, may result in negative feedback mechanisms, such as through USP11, which is known to inhibit Akt/mTOR signaling by upregulating PTEN [49]. This could enhance homeostasis and stop a tissue from rapidly depleting its nutrition supply [50].

In fact, prior research has demonstrated that PTEN expression can be elevated in early stages of cancer tissue, however in later stages, a down-regulation of PTEN relative to PI3K results in an over-activation of the Akt/mTOR pathway that promotes tumor growth. and metastases [51]. The most significant finding for the current investigation was the confirmation that, prior to co-culturing various cell lines, it is essential to examine common medium compositions in relation to their impacts on metabolic activity.Co-cultures with CCD-1137Sk fibroblasts were used to study the second point, which is the function of extracellular matrix for the development and proliferation of MDA-MB-231 spheroids. This produced conflicting outcomes. On the one hand, co-cultures of MDA-MB-231 and fibroblasts produced more spheroids than MDA-MB-231 monocultures in the absence of BME. However, in terms of spheroid formation speed, roundness, development, and long-term integrity, fibroblast co-cultures were unable to make up for the absence of BME. In fact, compared to BME-treated MDA-MB-231 mono-cultures, co-culture spheroids took longer to condense, developed less, and disintegrated more quickly over time in the absence of BME. This clearly implies that BME provides additional, as yet unidentified, elements that are advantageous for spheroid formation in addition to its supply of extracellular matrix components. Interestingly, MDA-MB-231 plus fibroblast co-cultures were smaller than MDA-MB-231 mono-cultures with equivalent numbers of MDA-MB-231 cells. Co-culture spheroids made from 10,000 fibroblasts and 10,000 MDA-MB-231 cells were, in fact, about the same size at 4 DIV as mono-cultures made from just 8,000 MDA-MB-231 cells.

There are now three possible explanations for this discovery because significant effects on cell proliferation might not be anticipated at this early stage. First, MDA-MB-231 cells may have died as a result of the co-culture, however after 4 DIV, there were no indications of many dead cells. Second, it's possible that the fibroblast cells prevented MDA-MB-231 cells from integrating into the spheroid culture, but we have no evidence to support this theory either. Lastly, fibroblasts may have caused MDA-MB-231 cells to become more compacted. A future study might focus on counting cells by kind in order to gain more understanding of these issues.One could contend that MDA-MB-231 mono-cultures are better for upcoming drug screening investigations given the previously noted uncertainties with co-cultures. However, cellular signaling between various cell types may also be significant for assessing possible drug efficacy in situ, even though spheroid integrity is undoubtedly a crucial quality for the simplicity of data extraction (see below). For instance, there is growing evidence that cancer and stroma cells in tumors interact metabolically [52], which could be a target for medications that target metabolism [53]. According to one line of research in this area, cellular communication in tumors may cause stromal fibroblasts to undergo an anabolic switch, which would produce lactate and possibly export it to feed nearby anabolic cancer cells [54]. Recently, this information was used to drive the tumor into a crucial energy-depleted condition through drug-induced metabolic tuning, making it more vulnerable to low doses of traditional chemotherapy therapies [55]. Therefore, these combination treatments may take advantage of tumor-specific metabolic changes to improve therapeutic efficacy and lessen adverse chemotherapeutic side effects. Nevertheless, it appears that in vitro test methods can only replicate such intricate interactions if the corresponding cell types are accessible.

Therefore, despite the previously described drawbacks of cancer-cell-fibroblast co-cultures, they may be required for the examination of such combinatorial effects. This was confirmed by our tests, which showed that MDA-MB-231 plus fibroblast co-cultures had differing levels of MCT4, a marker of lactate shuttling, and LC3-II, a measure of autophagic activity, compared to monocultures. Lastly, as with many other investigations, the results on spheroid shape that were provided demonstrated glaring variations in spheroid integrity over time and when comparing various culture modalities.

As a result, we strongly recommend using spheroid integrity as an indicator for data analysis based on spheroids. The application of random, manually analyzed spot assessments of core spheroid segmentations could be one strategy to address the problem of disaggregation and unfulfilled readout quality. A significant reevaluation of completely automated analysis utilizing software such as SpheroidSizer or other similar contrast-based methods is required if the integrity falls below a predetermined threshold value.Recognition We are grateful to Richard Schneider and Julia Meier-Hubberten of Merck KGaA, Darmstadt, Germany, for sharing the MDA-MB-231 cell line and for numerous insightful conversations. Finance The German Federal Ministry of Research (BMBF) provided funding for this project as part of the Innovation Partnership M2Aind (03FH8I01IA) under the "Starke Fachhochschulen – Impuls fu‘r die Region" (FH-Impuls) framework. The sponsoring organizations had no say in the study's design, data collection, analysis, or interpretation, or manuscript preparation. Contributions from authors Under the guidance of RR and MH, who both contributed to the studies by assisting with the organization and interpretation of the investigations, FK conducted the tests and prepared the report. Conflicts of interest There is no conflict of interest disclosed by the writers.

References

[1] Gilbert J, Henske P, Singh A. Rebuilding Big Pharma's Business Model: Big Pharma's successful business model is now irreversibly damaged. The sector requires a fresh strategy. The Business & Medicine Report, In Vivo, 2003.

[2] Wong CH, Siah KW, Lo AW. Clinical trial success rate estimation and associated parameters. Biostatistics, 2019, 20:273- 86. doi: 10.1093/biostatistics/kxx069

[3] Prasad V, Mailankody S. Research and development expenditures and post-approval income for a single cancer medication. JAMA Intern Med. 177:1569-75, 2017.

[4] Brinkley BR, Beall PT, Wible LJ, Mace ML, Turner DS, Cailleau RM doi: 0.1001/jamainternmed.2017.3601. differences in the cytoskeleton and cell shape of in vitro human breast cancer cells. Cancer Res. 40:3118-29, 1980.

[5] Cailleau R, Young R, Olive M, Reeves WJ. Pleural effusion-derived breast carcinoma cell lines. J Natl Cancer Inst. 1974;53:661-74.

[6] Pozo-Guisado E, Alvarez-Barrientos A, Mulero-Navarro S, Santiago-Josefat B, Fernandez-Salguero PM doi: 10.1093/jnci/53.3.661. Resveratrol's antiproliferative action causes MCF-7 human breast cancer cells to undergo apoptosis, but not MDA-MB-231 cells: cell-specific modification of the cell cycle. Biochemical Pharmacology, 64:1375-8, 20026. doi: 10.1016/s0006-2952(02)01296-0

[7] Hjortoe GM, Petersen LC, Albrektsen T, Sorensen BB, Norby PL, Mandal SK, et al. PAR-2 mediates tissue factor-factor VIIa-specific up-regulation of IL-8 production in MDA-MB-231 cells, which leads to enhanced cell migration.
Blood, 2004, 103:3029-37. doi: 10.1182/blood-2003-10-3417

[8] Pille J-Y, Denoyelle C, Varet J, Bertrand J-R, Soria J, Opolon P, et al. Anti-RhoA and anti-RhoC siRNAs prevent MDA-MB-231 breast cancer cells from proliferating and becoming invasive both in vitro and in vivo. Mol Ther. 2005;11:267-74. doi: 10.1016/j.ymthe.2004.08.029

[9] Viola M, Bruggemann K, Karousou E, Caon I, Carava E, Vigetti D, et al. Heparan sulfate, chondroitin-/dermatan sulfate, and hyaluronan biosynthesis interact intricately to control MDA-MB-231 breast cancer cell survival, motility, and matrix adherence. ATCC American Type Culture Collection

[10] Glycoconj J. 2017; 34:411-20. doi: 10.1007/s10719-016-9735-6. Protocol for Thawing, Propagating, and Cryopreservation; NCI-PBCF-HTB26 (MDA-MB-231) Breast Adenocarcinoma March 1, 2012. Manassas, VA20110, 1st ed.
[11] Cell Biolabs Inc. Product Data Sheet, MDA-MB-231/GFP Cell Line 2009, San Diego, CA 92126, 1st ed.
[12] Rozengurt E. Cell proliferation and growth factors. Current Cell Biology Opinion. 1992, 4:161-5. Schuldiner M, Yanuka O, Itskovitz-Eldor J, Melton DA, Benvenisty N. Effects of eight growth factors on the differentiation of cells produced from human embryonic stem cells
[13] doi: 10.1016/0955-0674(92)90027-A. Barnes D. Cell attachment and spreading factor assay. Proc Natl Acad Sci U S A. 2000;97:11307-12. doi: 10.1073/pnas.97.21.11307
[14]. Tissue Culture Methods Journal. 1986:69–74.
[15] Baker M. Reproducibility: Honor your cells! A co-culture model of the hippocampal neurogenic niche reveals distinct effects of astrocytes, endothelial cells, and pericytes on proliferation and differentiation of adult mouse precursor cells
[16] Ehret F, Vogler S, Kempermann G. Nature. 2016;537:433-5. doi: 10.1038/537433a. Stem Cell Res. 2015;15:514-21. doi: 10.1016/j.scr.2015.09.010
[17] Slavkin HC, Beierle J, Bavetta LA. Odontogenesis: Cell-cell interactions in vitro. Nature, 1968, 269-70.
[18] Noreen A, Rehman A, Shakoori AR, Aftab S. Tellurite-induced oxidative stress has an antiproliferative effect on breast cancer cells. 2019:68-75 J Cancer Res Pract.
[19] Hafner M, Heiser LM, Williams EH, Niepel M, Wang NJ, Korkola JE, et al. Quantification of sensitivity and resistance of breast cancer cell lines to anti-cancer medications using GR metrics doi: 10.4103/JCRP.JCRP 5 19.
[20] Liu Y-L, Chou C-K, Kim M, Vasisht R, Kuo Y-A, Ang P, et al. Evaluating metastatic potential of breast cancer cells based on EGFR dynamics. Sci Data. 2017;4:170166. doi: 10.1038/sdata. 2017.166.
[21] Picon-Ruiz M, Pan C, Drews-Elger K, Jang K, Besser AH, Zhao D, et al. Sci Rep. 2019;9:3395. doi: 10.1038/s41598-018-37625-0. Adipocytes and breast cancer cells interact to produce cytokines and promote the malignant development mediated by Src/Sox2/miR-302b. Cancer Res. 2016;76:491-504. doi: 10.1158/0008-5472.CAN-15-0927
[22] Hammerl A, Diaz Cano CE, De-Juan-Pardo EM, van Griensven M, Poh PSP. An osteoblast and peripheral blood mononuclear cell co-culture system devoid of growth factors for assessing the osteogenesis capability of melt-electrowritten polycaprolactone scaffolds. Int J Mol Sci. 2019. doi: 10.3390/ijms20051068
[23] Valkenburg KC, Groot AE de, Pienta KJ. improving cancer treatment by focusing on the tumor stroma.
[24] Martinez-Outschoorn UE, Pavlides S, Whitaker-Menezes D, Daumer KM, Milliman JN, Chiavarina B, et al. Nat Rev Clin Oncol. 2018;15:366-81. doi: 10.1038/s41571-018-0007-1. Implications for DCIS therapy with autophagy inhibitors and breast cancer: Tumor cells use caveolin-1 degradation to induce the cancer-associated fibroblast phenotype. Cell Cycle. 2010;9:2423-33. doi: 10.4161/cc.9.12.12048
[25] Wilde L, Roche M, Domingo-Vidal M, Tanson K, Philp N, Curry J, Martinez-Outschoorn U. Metabolic coupling and the Reverse Warburg Effect in cancer: Implications for the development of new biomarkers and anticancer agents. Semin Oncol. 2017;44:198-203. doi: 10.1053/j.seminoncol.2017.10.004

[26] Pavlides S, Vera I, Gandara R, Sneddon S, Pestell RG, Mercier I, et al. Warburg meets autophagy: Cancer-associated fibroblasts use oxidative stress, mitophagy, and aerobic glycolysis to speed up tumor development and metastasis. Signal of Antioxid Redox. 2012; 16:1264-84. doi: 10.1089/ars.2011.4243
[27] Kapałczynéska M, Kolenda T, Przybyła W, Zajań�czkowska M, Teresiak A, Filas V, et al. 2D and 3D cell cultures: a comparison of various cancer cell culture types.
[28] Breslin S, O'Driscoll L. Three-dimensional cell culture: The missing piece in drug development. Arch Med Sci. 2018;14:910-9. doi: 10.5114/aoms.2016.63743. Drug Discov Today. 2013; 18:240-9. doi: 10.1016/j.drudis.2012.10.003 [29] Bissell MJ, Rizki A, Mian IS. The final regulator of breast epithelial function is tissue architecture. Current Cell Biology Opinion. Mason BN, Starchenko A, Williams RM, Bonassar LJ, Reinhart-King CA
[30] 2003;15:753-62. doi: 10.1016/j.ceb.2003.10.016. Endothelial cell behavior is modulated by adjusting the stiffness of the three-dimensional collagen matrix without regard to collagen content. Acta Biomater. 9:4635-44 (2013). LaBonia GJ, Lockwood SY, Heller AA, Spence DM, Hummon AB
[31] doi: 10.1016/j.actbio.2012.08.007. Evaluation of irinotecan using MALDI imaging mass spectrometry: drug penetration and metabolism in 3D cell cultures treated in a 3D printed fluidic device. Liu X, Weaver EM, Hummon AB. Proteomics. 2016; 16:1814-21. doi: 10.1002/pmic.201500524
[32]. MALDI imaging mass spectrometry is used to assess treatments in three-dimensional cell culture systems. Anal Chem. 85:6295-302, 2013. doi: 10.1021/ac400519c
[33] Graf BW, Boppart SA. Three-dimensional cell culture model imaging and analysis. Methods Mol Biol. 2010;591:211-27. doi: 10.1007/978-1-60761-404-3 13
[34] Griffith LG, Swartz MA. capturing intricate 3D tissue physiology in vitro. Lin R-Z, Lin R-Z, Chang H-Y. Current developments in three-dimensional multicellular spheroid culture for biomedical research. Nat Rev Mol Cell Biol. 2006;7:211-24. doi: 10.1038/nrm1858
[35]. 2008; 3:1172-84; Biotechnol J. 10.1002/biot.200700228 is the doi [36] Hsiao AY, Tung Y-C, Kuo C-H, Mosadegh B, Bedenis R, Pienta KJ, Takayama S. Long-term spheroid culture in 384 hanging drop array plates is made possible by micro-ring structures that stabilize microdroplets. Microdevices for biomedicine. 2012;14:313-23. doi: 10.1007/s10544-011-9608-5
[37] Hongisto V, Jernstrom S, Fey V, Mpindi J-P, Kleivi Sahlberg K, Kallioniemi O, and Perella M. High-throughput 3D screening reveals variations in drug sensitivities between culture models of JIMT1 breast cancer cells. PLoS ONE. 2013;8:e77232. doi: 10.1371/journal.pone.0077232
[38] Kim JB, Stein R, O'Hare MJ. A review of three-dimensional in vitro tissue culture models of breast cancer. Treatment for breast cancer. 2004; 85:281-91.
[39] Harma V, Schukov H-P, Happonen A, Ahonen I, Virtanen J, Siitari H, et al. Quantification of dynamic morphological drug responses in 3D organotypic cell cultures by automated image analysis doi: 10.1023/B:BREA.0000025418.88785.2b. doi: 10.1371/journal.pone.0096426
[40] PLoS One, 2014, 9:e96426A high-throughput imaging and nuclear segmentation analysis technique for cleared 3D culture models by Boutin ME, Voss TC, Titus SA, Cruz-Gutierrez K, Michael S, and Ferrer M. Sci Rep. 8:11135, 2018. doi: 10.1038/s41598-018-29169- 0

[41] Chen W, Wong C, Vosburgh E, Levine AJ, Foran DJ, Xu EY. High-throughput image analysis of tumor spheroids: A user-friendly software tool to assess the size of spheroids automatically and correctly. J Vis Exp. 2014. doi: 10.3791/51639 [42] Maehama T, Dixon JE. Phos-phatidylinositol 3,4,5-trisphosphate is a lipid second messenger that is dephosphorylated by the tumor suppressor PTEN/MMAC1. J Biol Chem. 1998;273:13375-8. doi: 10.1074/jbc.273.22.13375
[43] Rustamov V, Keller F, Klicks J, Hafner M, Rudolf R. Early, high-proliferation stages of three-dimensional spheroid cell cultures of the breast cancer cell line MDA-MB-231 exhibit increased expression of bone sialoprotein. Front Oncol. 2019;9:36. doi: 10.3389/fonc.2019.00036
[44] Kabeya Y, Mizushima N, Ueno T, Yamamoto A, Kirisako T, Noda T, et al. After processing, LC3, a human homologue of yeast Apg8p, is found in autophagosome membranes. EMBO J. 2000;19:5720-8. doi: 10.1093/emboj/19.21.5720
[45] Burguera EF, Bitar M, Bruinink A. In vitro co-culture technique to study heterotypic cell-cell interactions. eCM. 2010;19:166-79. doi: 10.22203/eCM.v019a17
[46] Yamaguchi Y, Kudoh J, Yoshida T, Shimizu N. In vitro co-culture methods for investigating the molecular basis of cellular interaction between fresh thymocytes and medullary thymic epithelial cells that express Aire. 2014; 3:1071-82, Biol Open. Langhans SA. Three-dimensional in vitro cell culture models in drug discovery and drug repositioning
[47] doi: 10.1242/bio.201410173. Front Pharmacol. 2018;9:6. doi: 10.3389/fphar.2018.00006
[48] Soule HD, Maloney TM, Wolman SR, Peterson WD, Brenz R, McGrath CM, et al. Isolation and characterization of MCF-10, a spontaneously immortalized human breast epithelial cell line. Cancer Res. 50:6075-86, 1990.
[49] Park MK, Yao Y, Xia W, Setijono SR, Kim JH, Vila IK, et al. PTEN stabilizes tumor suppression by self-regulating via USP11 via the PI3K-FOXO pathway.
[50] Edinger AL. Nat Commun. 2019;10:636. doi: 10.1038/s41467-019-08481-x. regulating the expression of nutrient transporters to control cell growth and survival. Biochem J. 406:1-1, 20072. doi: 10.1042/BJ20070490
[51] Zeleniak AE, Huang W, Fishel ML, Hill R. PTEN-dependent stability of MTSS1 suppresses the metastatic phenotype in pancreatic ductal adenocarcinoma. Neoplasia. 2018; 20:12-24. doi: 10.1016/j.neo.2017.10.004
[52] Denton AE, Roberts EW, Fearon DT. Tumor microenvironment stromal cells. Adv Exp Med Biol. 2018; 1060:99-114. doi: 10.1007/978-3-319-78127-3 6
[53] Fu Y, Liu S, Yin S, Niu W, Xiong W, Tan M, et al. The reverse Warburg effect is probably one of cancer's weaknesses that can be used to treat the disease. Oncotarget. 2017; 8:57813-25. doi: 10.18632/oncotarget.18175
[54] Martinez-Outschoorn UE, Pavlides S, Howell A, Pestell RG, Tanowitz HB, Sotgia F, Lisanti MP. Autophagy and metabolism in the tumor microenvironment are integrated in stromal-epithelial metabolic coupling in cancer. Int J Biochem Cell Biol. 43:1045-51, 2011. doi: 10.1016/j.biocel.2011.01.023
[55] Maycotte P, Thorburn A. Autophagy and cancer treatment. Biol Therapy for Cancer. 2011; 11:127–37. 104161/cbt.11.2.14627 is the doi